Antifungal and mucoadhesive properties of an orally administered chitosan-coated amphotericin B nanostructured lipid carrier (NLC)

AAPS PharmSciTech

Janet Tan Sui Ling[1], Clive Roberts[2] and Nashiru Billa[1*]

Running head: An oral antifungal Amphotericin-B NLC

ABSTRACT

Surface - modified nanostructured lipid carriers (NLC) is a promising formulation to prolong the retention time of the therapeutic agent at the site of absorption. Chitosan-coated AmpB-loaded NLC (ChiAmpB NLC) were developed showing particle size of 394.4 ± 6.4 nm, encapsulation efficiency of 86.0 ± 0.3 % and a drug loading of 11.0 ± 0.1 %. ChiAmpB NLC showed biphasic release behaviour with no significant change in its physical properties upon exposure to conditions simulating the gastrointestinal tract. Compared to pure AmpB, ChiAmpB NLC observed not only a comparable antifungal behaviour but showed superior safety profiles, with two times lesser toxicity to the red blood cells and ten times safer to the HT-29 cell line. It was also successfully observed a translation of the *in vitro* mucoadhesion result to the *ex vivo* animal study in which ChiAmpB NLC results in higher percentage of retention in the small intestine compared to uncoated formulation. Together, the data strongly offered the possibility of having a non-toxic yet effective oral treatment for systemic fungal infections.

INTRODUCTION

Disseminated fungal infections account for 30 % of death in patients with weakened immune system, especially in those with cancer, HIV / AIDS and organ transplant patients (1,2). Despite the recent discovery of new antifungal agents, amphotericin B (AmpB) remains the gold standard for the treatment of invasive fungal infections (3).

AmpB is currently administered intravenously stabilised in micelles or liposomes (Fungizone ®, Ambisome ®, Abelcet ® and Amphocil ®) and although effective, patients have to contend with severe side effects such as haemolysis, anaemia, fever, headache and kidney toxicity attributable to the mechanism of action of AmpB and the excipients in the formulation (4,5). Furthermore, drawbacks in terms of safety and cost means that this mode of delivering AmpB is not sustainable.

Oral administration of AmpB has been recognised as a potential strategy of minimizing the side effects experienced by patients with the above formulations (6–12). However, attempts to formulate oral delivery system for AmpB have yet to be translated to the clinic. This impasse is mainly due to the physicochemical properties of AmpB, such as high molecular weight (924 Da), zwitterionic and amphipathic characteristics in addition to the asymmetrical distribution of hydrophobic and hydrophilic groups (13,14). Thus, oral administration of AmpB results in low bioavailability (<0.3 %), precluding any therapeutic usefulness to patients (12,15).

Nanostructured lipid carriers (NLC) ~~is~~ are the second generation solid lipid nanoparticles (SLN) derived from admixture of solid lipid and liquid oil. NLC presents a combination of controlled drug release, high drug loading, good biocompatibility and stability (16,17). Due to the advantages offered by the NLC, there are attempts by researchers to encapsulate AmpB within NLC (18–21). Orally

administered dosage forms may present a short transit at the absorption window within the duodenum and in such cases, absorption is not maximised. Prolonged gastrointestinal retention at the site of absorption may improve the chances of uptake/absorption across the epithelium. Bioavailability is potentially improved so that the need for multiple administrations is negated (22,23). Surface modification of dosage forms using synthetic or natural polymers may be used to delay their transit within the gastrointestinal tract and possibly, maximise uptake as presented above (24). Chitosan is a natural cationic polymer with documented mucoadhesive properties (25). It has successfully been used to promote the *in vivo* absorption of insulin-loaded SLN via its mucoadhesive effect in the gastrointestinal tract (26). Besides, chitosan-coated NLC showed a delay in the ocular clearance and an improved bioavailability of flurbiprofen compared to the uncoated NLC (22).

We previously reported on the design of both uncoated and chitosan-coated AmpB-loaded NLC (18). Although in general, NLC and chitosan meet the pre-requisites as safe nanocarriers, the clinical evidence for this safety, whilst crucial, is not always manifest in scientific reports (27–29). The present endeavour is aimed at deciphering the potential of the formulation as an oral delivery system of AmpB and subsequently, the effectiveness and toxicity of the formulation.

MATERIALS AND METHODS

Materials

Amphotericin B was obtained from Fisher Scientific, India. The commercial formulation of amphotericin B deoxycholate (Amphotret®, Bharat Serums and Vaccines Limited, India) was a gift from Pahang Pharmacy, Malaysia. Beeswax and coconut oil were from Acros Organics, New Jersey, USA. Chitosan, (low molecular weight), phosphate buffered saline tablets (PBS), RPMI-1640 without L-glutamine and 3-(N-Morpholino) propanesulfonic acid (MOPS) were purchased from Sigma Aldrich Co. LLC., Missouri, USA. Soya lecithin was purchased from MP Biomedicals (Illkirch, France) and acetic acid was obtained from R&M Chemicals, India. Dulbecco's Modified Eagle's Medium (DMEM)

was purchased from Nacalai Tesque Inc., Kyoto, Japan while Foetal Bovine Serum (FBS) was obtained from Tico Europe, Netherlands. All reagents and solvents used of analytical and HPLC grades respectively. Deionised water used was Milli-Q 18.2 MΩ.cm at 25 °C (Millipore Corp., Bedford, USA).

Formulation of chitosan-coated AmpB-loaded NLC (ChiAmpB NLC) formulation

AmpB-loaded NLC (AmpB NLC) was formulated by combination of homogenization and ultrasonication techniques as previously described (18). Briefly, 290 mg of beeswax and 10 mg of coconut oil were heated to 70 °C before the addition of AmpB. At the same time, 50 mg of Tween-80 and 50 mg of lecithin were mixed with 10 mL of deionised water and stirred at 70 °C at 500 rpm for 45 minutes. The surfactant mixture was added into the melted lipids containing AmpB before being homogenized at 12 400 rpm for 8 minutes using high speed homogenizer (Ultra-Turrax T25, Germany). The coarse emulsion was further subjected to probe ultrasonication (Q500 QSonica, Newtown, CT, USA) for further 8 minutes at 20 % amplitude. The mixture was poured into 4 °C deionised water under 500 rpm of stirring, making up a total of 100 mL. Chitosan (dissolved in 1 % v/v acetic acid) was added in a dropwise manner into the formed AmpB NLC in 1: 40 v/v under stirring of 250 rpm or 15 minutes. Drug-free ChiNLC formulations were prepared as above but with the omission of AmpB.

Characterisation of the formulations

The particle size (z-average), polydispersity index (PDI) and zeta potential (ζ) were studied using the Zetasizer Nano ZS® (Malvern Instruments, UK) equipped with a 4-mV He-Ne laser at a wavelength of 633 nm. All samples were diluted in 1:20 v/v using deionised water and measurements were carried out in triplicate at 25 °C and the results were expressed as mean ± standard deviation. Chemical transformations in chitosan, chitosan-coated NLC and NLC were assessed using Fourier transform infrared – attenuated total reflection (FTIR-ATR) equipped with ATR sampling accessory with a diamond crystal (Perkin Elmer, Waltham, USA). The freeze-dried

formulations were placed directly to the ATR compartment and the spectra were recorded from 400 - 4000 cm^{-1} at a resolution of 1 cm^{-1}.

Free AmpB was removed after precipitation of the formulation using acetonitrile, followed by centrifugation at 20 000 rpm for 10 minutes at 4 °C. The pellet containing the encapsulated AmpB was dissolved in DMSO:MeOH (1:1) and heated at 70 °C. The amount of AmpB entrapped within the particles was measured using an HPLC system (1260 Series, from Agilent technologies, Waldbronn, Germany, equipped with a 15 cm x 4.6 mm reversed-phase C-18 column, Hypersil Gold, ThermoFisher Scientific, Waltham, United States, 5 µm particle size stationary phase). Results are expressed as mean ± standard deviation. The linear regression of the calibration curve was obtained for AmpB at a concentration of 0.1-100.0 µg/mL in DMSO: MeOH (408 nm) with r^2 of 0.9998. The encapsulation efficiency and drug loading were calculated as the following equations:

$$\%EE = \frac{W_S}{W_T}100 \quad \text{..... (1)}$$

$$\%DL = \frac{W_S}{W_N}100 \quad \text{..... (2)}$$

where, W_T is the amount of AmpB in the system, W_S is the amount of AmpB detected in the sediment and W_N weight of nanoparticles obtained from freeze-dried sediments.

Physical stability studies

The formulations were stored at 4 °C and protected from light. After 15 months' storage, aliquots were withdrawn and the particle size, PDI, ζ and encapsulation efficiency were evaluated.

In vitro studies

Amphotericin B release and stability studies

The release of AmpB from ChiAmpB NLC was examined in relevant release medium (PBS, pH 7.4 containing 1% Tween-80) where release of free AmpB in DMSO: MeOH was used as a control.

Briefly, 50 µL of fresh ChiAmpB NLC formulation was mixed with 950 µL of release medium and gently shaken in rotary shaker (WiseCube®, Witeg Inc., Germany) at 37 °C. Tubes were removed at predetermined time intervals (15 min, 1, 2, 3, 4 and 5 hour), centrifuged at 20,000 rpm for 10 minutes at 4 °C. ~~and t~~The amount of AmpB released was determined by analyzing the supernatants using the HPLC system described above. The experiment was carried out in triplicate and results were expressed as mean ± standard deviation. The amount of AmpB released was calculated as follows:

$$\text{Release of AmpB (\%)} = \frac{W_R}{W_S}100 \quad \text{.....(3)}$$

where, W_S is the amount of AmpB detected in the sediment and W_R is the amount of AmpB released in the supernatant.

The stability of the formulation in pH conditions simulating the relevant sections of the gastrointestinal tract was investigated by adding 50 µL of ChiAmpB NLC to 950 µL of acidic (pH 1.2, USP), near-acidic (pH 5.8, BP) or near-neutral (pH 6.8, BP) media representing the stomach, proximal and distal duodenum. The mixture was incubated at 37 °C and rotated at 120 rpm in rotary shaker (WiseCube®, Witeg Inc., Germany) for 2 hours. Aliquots were withdrawn from each medium and evaluated in terms of particle size and ζ as described above.

Mucoadhesion studies

A fall in ζ values was used as a measure of the extent of mucoadhesion between the formulations and mucin. This provided an insight of the mucoadhesive propensity of the formulation at relevant region within the gastrointestinal tract (30,31). The mucin used was type III porcine gastric mucin dispersed in pH 5.8 and 6.8 media (BP) under mild stirring at a concentration of 0.05, 0.1, 0.25, 0.5, 0.75, 1.0 % w/v. Aliquots of formulations were mixed with each mucin concentration at 1:1 v/v ratio. The mixture was incubated at 37 °C for 2 hours in rotary shaker (WiseCube ®, Witeg Inc., Germany) operated at 120 rpm. The change in the ζ values was measured using the Zetasizer

Nano ZS® (Malvern, UK) after appropriate dilution. Measurements were performed in triplicate and results were expressed as mean ± standard deviation.

Antifungal studies

The broth microdilution method was used to determine the minimum inhibitory concentration (MIC) of the formulation against *Candida albicans* (ATCC 90028) and based on the Clinical Laboratory Standards Institute (CLSI) guideline (M-27A). The broth medium was Roswell Park Memorial Institute (RPMI) 1640 with 0.165 M of MOPS [3-(N-morpholino) propanesulfonic acid]. The *Candida albicans* was grown aerobically in Sabouraud dextrose agar at 35 °C for 24 hours. The yeast inoculum was prepared by picking 5 colonies and suspended in 5 mL of sterile saline and the cell density was adjusted in accordance with 0.5 McFarland standard. The yeast suspension was diluted 1:50 in sterile saline and further diluted 1:20 in broth medium, resulting in 0.5×10^3 to 2.5×10^3 CFU/mL. 100 µL of the yeast suspension was loaded into the wells of the 96-well plates containing 100 µL of AmpB resulting in final concentration of AmpB of 0.03125 – 16 µg/mL (Row 1-10). AmpB dissolved in DMSO was used as control. The stock solution of AmpB in DMSO was diluted using the broth medium, reducing the concentration of DMSO to 1%. Row 11 and 12 of the wells were used as controls; medium only and medium with yeast inoculum. The plates were incubated at 35 °C for 48 hours. The MIC were determined at 24 and 48 hours by measuring the absorbance of the samples at 530 nm using a UV-visible spectrophotometer (Epoch Microplate Spectrophotometer, Bio Tek Instruments, USA). Experiments were run in triplicate and results were expressed as mean ± standard deviation.

Toxicity studies

Haemolysis study

Fresh blood samples were obtained from three healthy Sprague-Dawley male rats via cardiac puncture and erythrocytes (RBCs) were isolated by centrifugation at 3000 rpm for 10 minutes at 4 °C. The supernatant along with buffy coat were pipetted and discarded. RBCs were washed thrice with phosphate buffered saline (PBS, pH 7.4) and dispersed in fresh PBS to obtain a 1 % haemotocrit. 300 µL of the RBCs suspension was mixed with 300 µL of the formulations, giving final AmpB concentration in a range of 6.25 - 100 µg/mL. Pure AmpB dissolved in DMSO was used as control in which the final concentration of DMSO was reduced to < 0.01 % v/v using PBS. Deionised water with 0.1 % v/v Triton-X was used as positive control (100 % haemolysis) while PBS solution was utilised as negative control (0 % haemolysis). The mixture of RBCs and formulations was incubated at 37 °C in a rotary shaker (WiseCube ®, Witeg Inc., Germany) at 100 rpm. The experiment was performed in triplicate. After predetermined time interval of incubation, any haemolysis was stopped by immersion of the sample tubes into ice water bath (0 °C) and unlysed RBCs were removed by centrifugation at 3000 rpm for 10 minutes. The haemoglobin released in the supernatant was collected and absorbance measured at 580 nm using a UV-visible spectrophotometer (Epoch Microplate Spectrophotometer, Bio Tek Instruments, USA) (32,33). The percentage of haemolysis was calculated according to the following equation.

$$\text{Haemolysis (\%)} = \frac{Abs_s - Abs_0}{Abs_{100} - Abs_0} 100 \quad \text{..... (4)}$$

where, Abs_s is the absorbance of the sample, Abs_0 is the absorbance of 0 % lysed sample treated with PBS (pH 7.4) and Abs_{100} is the absorbance of 100 % lysed sample treated with deionised water with 0.1 % v/v Triton X-100.

Cytotoxicity study

The cytotoxicity effect of the formulations was evaluated against HT-29 cells using 3-(4,5-Dimethylthiazol-2-yl)-2,5-Diphenyltetrazolium bromide (MTT) assay. A 200 µL aliquot of cell suspension was seeded into 96-well plate at 5000 cells per well and incubated for 24 hours at 37 °C

prior to drug treatment. The culture medium was replaced with 180 µL of fresh media before adding 20 µL of formulations, achieving final concentration of AmpB in a range of 6.25 - 100 µg/mL. The mixture was incubated at 37 °C, 70 % humidity and 5 % carbon dioxide. Pure AmpB dissolved in DMSO were also studied with the final concentration of DMSO being reduced to 0.01 %v/v. Pure medium and medium containing cells were used as negative controls. At predetermined time interval of incubation, 20 µL of MTT solution (5 mg/mL) was added and the mixture was further incubated for 4 hours at 37 °C. The medium was removed and 100 µL of DMSO was added to dissolve the formazan crystals. The cell viability was assessed by measuring the absorbance of the solution at a wavelength of 570 nm (Epoch Microplate Spectrophotometer, Bio Tek Instruments, USA) with 630 nm used as reference wavelength. The cell viability was calculated based on the equation below.

Cell viability (%) = $\frac{Abs_S}{Abs_C}$ 100……. (5)

where, Abs_s is the absorbance obtained from the sample and Abs_c is the absorbance obtained from the control.

Animal study

Ex vivo intestinal adhesion studies

An *ex vivo* mucoadhesion study was conducted on excised intestinal tissue of rats so as to further validate the *in vitro* studies above. Six Sprague-Dawley male rats weighing 250-300 g were sacrificed and intestinal tissue excised. The animals used for the study were obtained from the animal house facility of the University of Putra Malaysia with prior approval from Animal Welfare and Ethical Review Body of University of Nottingham, UK (UMNC 19). Six centimetres of the jejunum was flushed with 10 mL of ice-cold phosphate buffer and everted using stainless steel rod. Both ends of the jejunum segment was ligated and the sac was filled with 1.5 – 2 mL of Dulbecco's Modified Eagle's Medium (DMEM). The tissue was immersed in a 50 mL centrifuge tube containing 5 mL of

DMEM and maintained at 4 °C. 10 mL of formulation was added into the tube and was incubated at 37 °C for 30 minutes at 120 rpm in rotary shaker (WiseCube ®, Witeg Inc., Germany). The uncoated formulation was used as control. The sac was removed and the content in the tube was precipitated using acetonitrile, centrifuged at 10 000 rpm for 15 minutes and washed with deionized water. The precipitate was lyophilised and the unbound nanoparticles were weighed. The percentage of bound nanoparticles was calculated using the following equation:

$$\text{Binding (\%)} = \frac{W_N - W_U}{W_N} 100 \quad \text{..... (6)}$$

where, W_N is the initial weight of the nanoparticles and W_U is the weight of the unbound nanoparticles. The animal used in this phase of the work were fresh cadavers used in a separate investigation so that no animals were sacrificed solely for this work. An Ethical Clearance was sought prior to commencement of the work, nonetheless.

Statistical analyses

Statistical evaluation was performed using one-way analysis of variance (ANOVA), Tukey's post hoc test was conducted for multiple comparison between groups and differences were considered significant when $p < 0.05$. All calculations were conducted using IBM SPSS Statistics 24 (IBM cooperation, New York, NY).

RESULTS AND DISCUSSION

Figure 1 shows the FTIR-ATR spectra of pure chitosan, NLC and ChiNLC formulations. The characteristic bands for chitosan were observed at 3284, 1646 and 1557 cm^{-1} indicating a stretching of –OH groups, C=O from amide I, N-H bending and C-N stretching from amide II, respectively (23,31,34). In contrast to the NLC, we observed two distinctive peaks of amide I and II at 1635 and 1539 cm^{-1} for ChiNLC. These two peaks are slightly shifted compared to those from pure chitosan. Hence, we inferred that the adsorption of chitosan was due to interactions between the amino

group of the chitosan with the ester groups of the lipids. These findings are in accordance with results from other researchers (23,34).

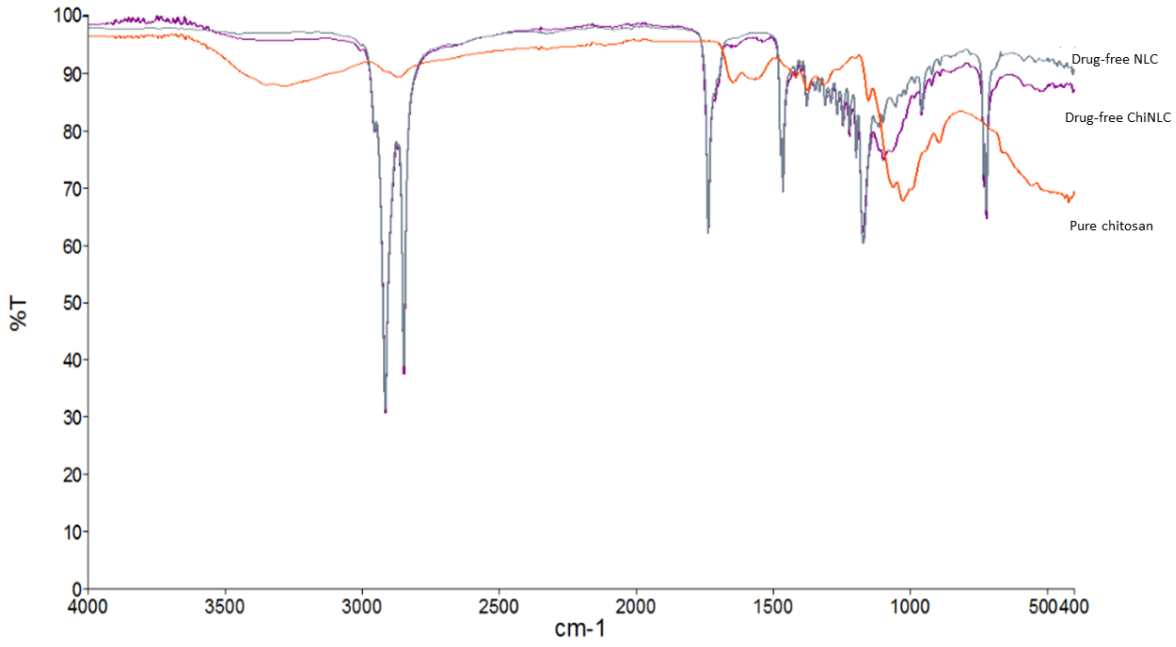

Figure 1: FTIR-ATR spectra of (from top) drug-free NLC, drug-free ChiNLC and pure chitosan

Both AmpB-loaded and drug free formulations of chitosan-coated NLC were evaluated based on particle size, polydispersity index (PDI), zeta potential (ζ), encapsulation efficiency and drug loading as shown in Table 1.

Physical Properties	ChiNLC	ChiAmpB NLC	
	Fresh	Fresh	15 months
Particle size (nm)	322.5 ± 4.5	394.4 ± 6.4*	231.0 ± 5.6*
PDI	0.44 ± 0.03	0.44 ± 0.03	0.42 ± 0.03
Zeta potential (mV)	26.5 ± 0.4	18.8 ± 0.3*	9.8 ± 0.3*
Encapsulation efficiency (%)	-	86.0 ± 0.3	79.8 ± 0.3*
Drug loading (%)	-	11.0 ± 0.1	10.2 ± 0.03

*p<0.05: statistical significance between fresh ChiAmpB NLC and 15-month formulation (mean ± S.D., n=3)

Upon incorporation of AmpB, there was an increase in size of the ChiNLC from 322.5 ± 4.5 to 394.4 ± 6.4 nm in accordance with reports from other studies (28,35). In general, aggregation of particles is often observed upon storage of nanoformulations where the systems move to stabilised states by lowering their surface area to volume ratio (36). Interestingly, the ChiAmpB NLC presented a lower size range and PDI value after 15 months of storage. This change could attributed to rearrangement of the chitosan layer, which resulted in the formation of a more condensed particle (8,37). However, we cannot eliminate the possibility of some dissociation of the chitosan layer as well since a decrease in ζ was observed. Notwithstanding, the ChiAmpB NLC remained positively charged during the 15-month storage, which points to the retention of sufficient chitosan coating, enough to retain electrostatic repulsion and size. Previous studies have reported that cationic nanoparticles were easily attracted to negatively charged endothelial cells which further ease the absorption of the particles (38,39). Both ChiNLC and ChiAmpB NLC presented a positive ζ, which indicate that chitosan was successfully adsorbed onto the surface of the NLC formulations (34). Although ChiAmpB NLC registered a significant reduction in the ζ values after 15-month of storage, we believe that adequate electrostatic repulsion was maintained since the size of the formulation remained in the nano-range. Thus, the formulation appears stable and therefore suitable to be developed into oral delivery system (Table 1). The encapsulation efficiency of the ChiAmpB NLC was 86.0 ± 0.33 % whilst the drug loading was 11.0 ± 0.1 % (Table 1). The high encapsulation efficiency and drug loading can be attributed to the crystal disorder offered by the liquid oil within the solid lipid, providing enough space to accommodate the AmpB (40–42). The disordered structure also prevents crystal growth so that expulsion of AmpB was checked during storage, with only 6.2 % expulsion after 15 months.

The *in vitro* AmpB release studies were conducted in phosphate buffer with 1% Tween-80 to maintain sink condition and the release profile of the formulations are depicted in Figure 2.

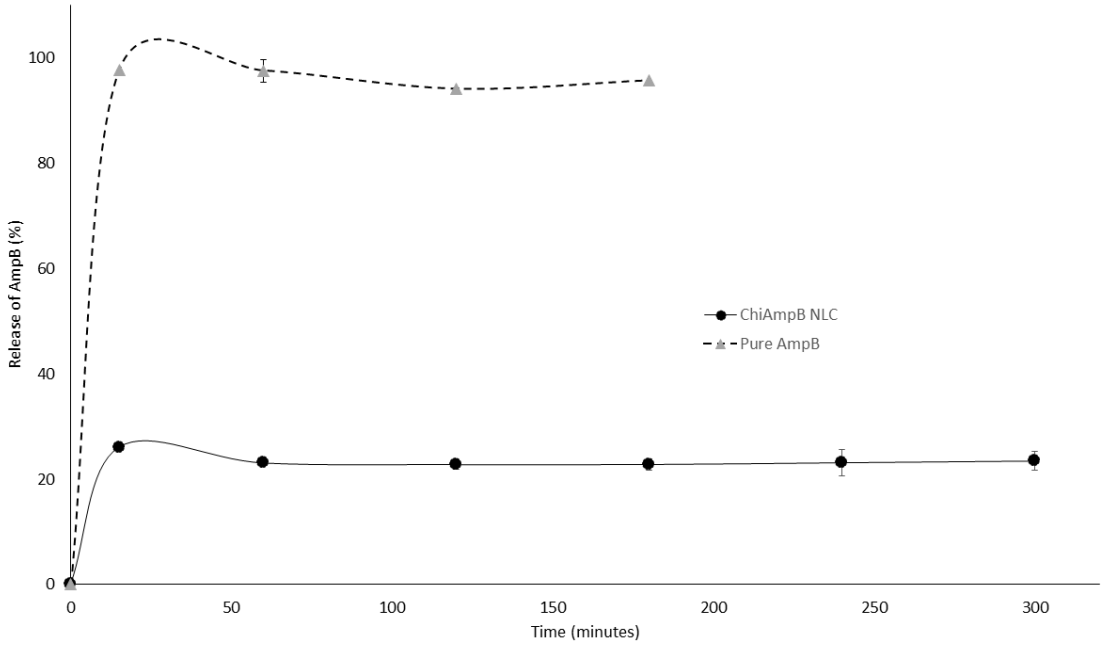

Figure 2: *In vitro* AmpB release from ChiAmpB NLC formulation and free AmpB. [mean ± S.D. (n=3)]

The release of pure AmpB was used as a control and exhibited a rapid release of up to 100 % within 15 minutes. On the other hand, the ChiAmpB NLC showed biphasic release profiles, with burst release (27 %) observed within the first 15 minutes followed by a more extended release over 5 hours, which is in accordance with other studies (43–45). We hypothesized that the burst effect observed was due to degradation of the thin chitosan coating (46) while the second phase of release corresponds to the diffusion of the AmpB from the lipidic core (47). The sustained release pattern of the ChiAmpB NLC was best fitted into zero order release model (r^2 = 0.904) as compared to other mathematical models (first order, Higuchi and Korsemeyer-Peppas) (43). This profile is in accordance with studies by other researchers (43–45). The effect of variation in pH simulating the gastrointestinal tract on the changes in the physical properties of ChiAmpB NLC in terms of particle

size and ζ is presented in Figure 3. pH 1.2 comprised of 0.03 M NaCl and 0.1 M HCl, portraying the dominant electrolyte of the gastric.

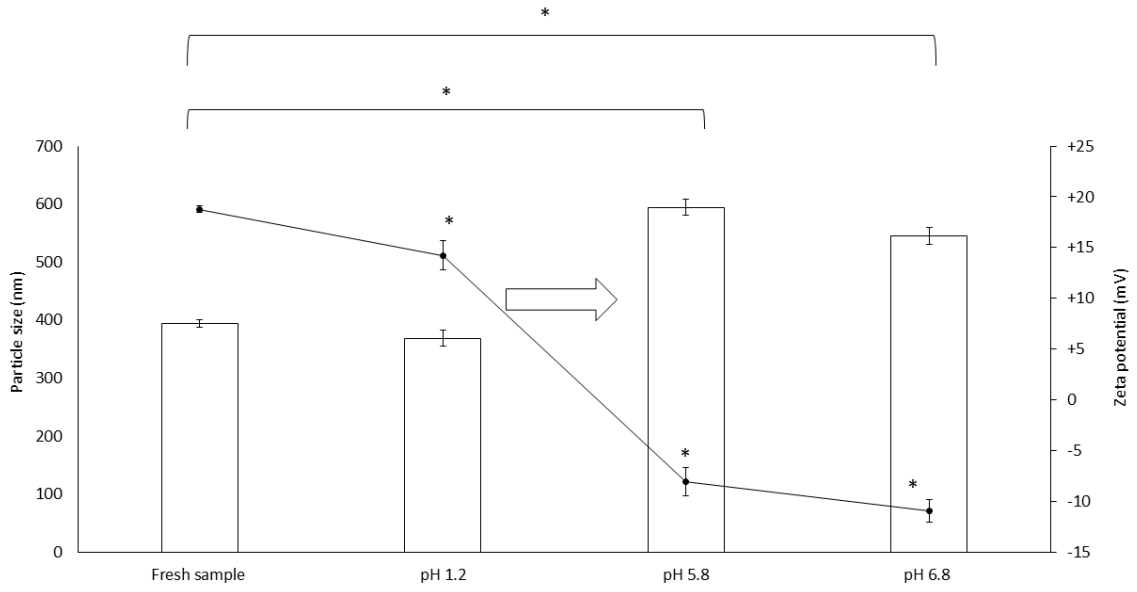

Figure 3: Particle size and ζ of ChiAmpB NLC before and after exposure to simulated GI fluids [mean ± S.D., n=3; *p < 0.05, significantly different with the fresh sample]

No significant change in the particle size was observed after the exposure of ChiAmpB NLC to pH 1.2 for 2 hours (p = 0.138). At pH 5.8 and 6.8, the particle size increased significantly to 594.5 ± 14.5 and 544.9 ± 14.6 nm respectively. However, this should not be a concern as the sizes remain in nanometre range. The ChiAmpB NLC showed a slight drop in ζ upon exposure to pH 1.2 followed by a significant decrease, reversing from positive ζ to negative upon exposure to pH 5.8 and 6.8. This reversal in magnitude of ζ is likely to impede mucoadhesion with cells, however exposure to acidic pH can be controlled through enteric encapsulation of the ChiAmpB NLC. This indicates the

neutralisation of the positive charge on the fresh ChiAmpB NLC by the anions present in the phosphate buffer which further led to the increase in particle size observed (48).

Figure 4 shows the change in the ζ values of ChiAmpB NLC after incubation in mucin solutions maintained at various pH. Mucin is negatively charged due to the presence of sialic acid while the ChiAmpB NLC has a positive ζ prior incubation due to the amine groups in chitosan as described earlier.

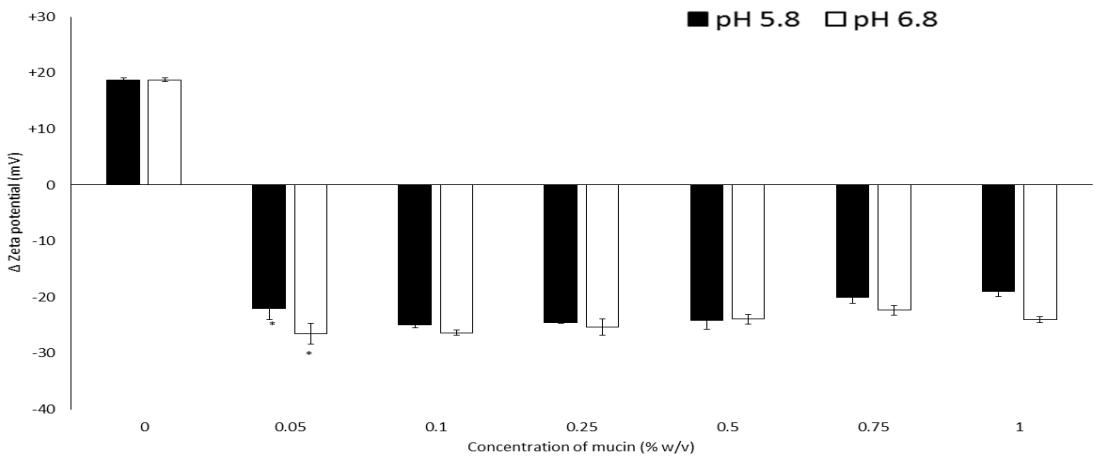

Figure 4: *In vitro* mucoadhesion in simulated intestinal pH [mean ± S.D., n=3; *p < 0.05, significantly different from fresh sample and 0.05 %w/v mucin in pH 5.8 and 6.8]

Any decrease in ζ value of the formulation will indicate interaction between amine groups of chitosan with mucin and reflecting mucoadhesive properties of ChiAmpB NLC (30). The ChiAmpB NLC showed a significant drop in ζ values in both pH conditions; from +18.8 ± 0.3 mV to -22.1 ± 0.3 (pH 5.8) and -26.5 ± 0.3 mV (pH 6.8) at 0.05 % w/v mucin concentration, thus confirming the mucoadhesive propensity of the ChiAmpB NLC formulation. Noteworthy, a higher drop in ζ values was observed at pH 6.8 (Figure 4), reflecting stronger mucoadhesive properties of the ChiAmpB NLC formulation at this pH. This can be explained based on the variation in pH and charge of the mucin. Mucin has a pKa of 2.6 which was highly negatively charged at pH 6.8. This allowed the ionised

functional groups of -$COOH^-$ of mucin to repel each other, making them more accessible for interactions with cationic moieties such as -NH_3^+ groups of chitosan which thus, resulted in stronger mucoadhesive effects (31,49).

An *ex vivo* mucoadhesion study was also conducted as it will provide a direct insight on the behaviour of the formulation with a biological substrate presented as freshly excised small intestine of the rats (30). The uncoated AmpB NLC formulation was used as a control and ChiAmpB NLC formulation showed an 84.2 ± 5.1 % adhesion to the intestinal lining of the rats (Figure 5).

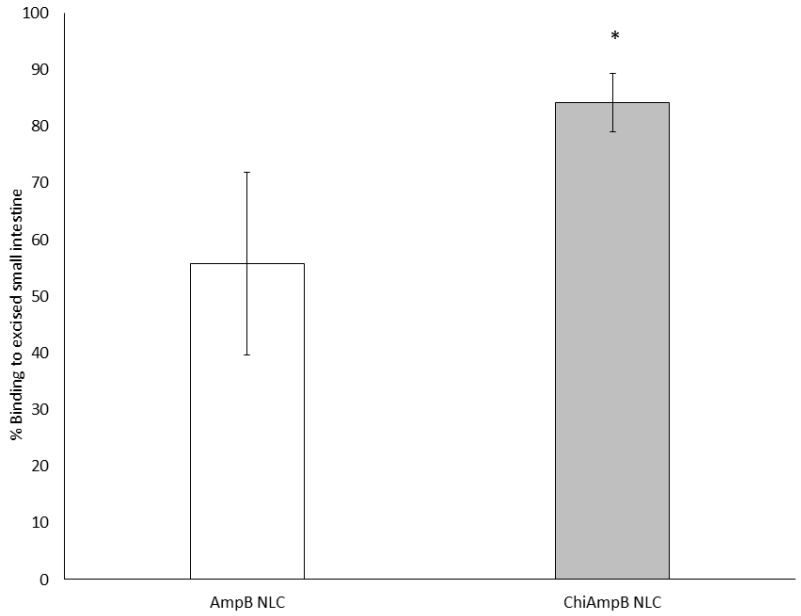

Figure 5: *Ex vivo* mucoadhesion assay using everted intestinal sac. [*p < 0.05: significant difference between chitosan-coated and uncoated AmpB NLC formulations (mean ± S.D., n = 6]

In contrast, the uncoated AmpB NLC showed 55.8 ± 16.1 % binding of nanoparticles upon incubation with everted intestinal sac of rats. This affirms the mucoadhesive propensity of ChiAmpB NLC which is attributable to the chitosan coating so that prolonged contact time with the intestinal would assure prolonged transit and hence enhanced ChiAmpB NLC uptake (39).

The antifungal efficacy of the formulations was studied against the *Candida albicans* which is one of the predominant causative agents in systemic fungal infections. The minimum inhibitory

concentration (MIC) values of the standard (AmpB in DMSO) were 0.25 and 0.5 µg/mL after 24 and 48 hours, respectively which is in accordance with the other studies (32,33). Thus, it can be reasonably inferred that AmpB with concentration of < 0.5 µg/mL exhibited fungistatic effect while > 0.5 µg/mL portrayed fungicidal behaviour. The drug-free ChiNLC did not elicit any antifungal behaviour. On the other hand, the MIC values of the ChiAmpB NLC mirror those from the standard, exhibiting 0.25 and 0.5 µg/mL after 24 and 48 hours, respectively. We may conclude that the antifungal efficacy of the AmpB was retained and not altered by the formulation processes.

Haemolysis is one of the major toxicities manifested by AmpB which hinders its clinical applications. In our previous reports (9,18), we have proposed the possibility of delivering the nano-carrier via the lymphatic route. Therefore, the likelihood of emptying intact ChiAmpB NLC to the systemic circulation is plausible. This warrants investigation on how the blood might respond to the formulation via a haemolysis study. The haemolysis of the pure AmpB was significantly higher than all the formulations studied, showing a minimum of 80 % haemolysis at concentration as low as 6.25 µg/mL upon 3-hour incubation (Figure 6).

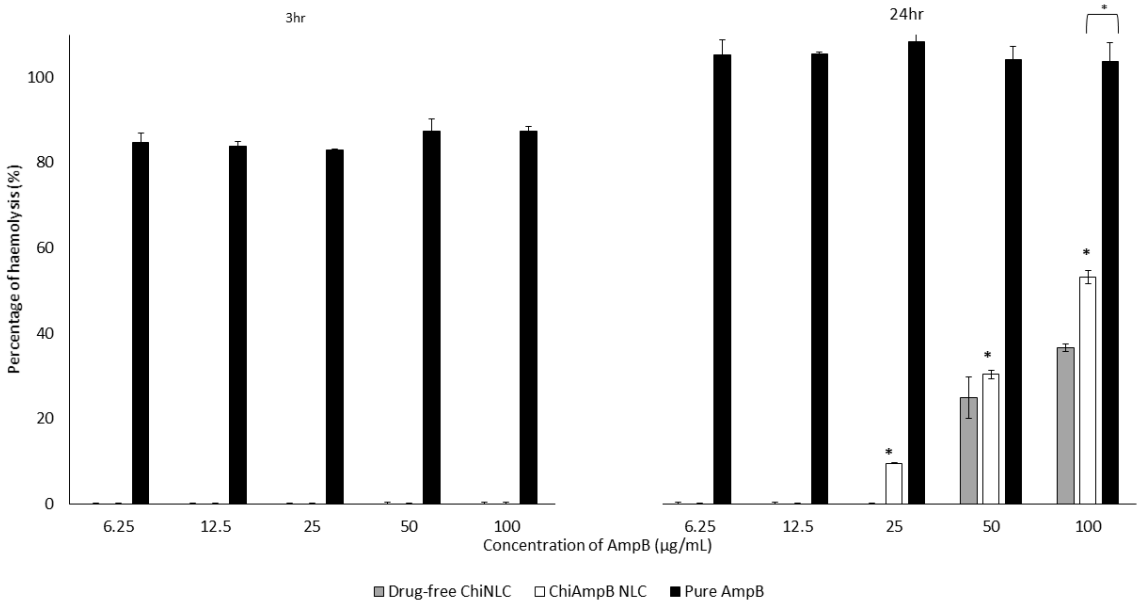

Figure 6: Percentage haemolysis of formulations after 3 and 24-hour of incubation [mean ± S.D., n=3. *p<0.05: significant difference between percentage haemolysis of 1) ChiAmpB NLC at 3 and

24-hour incubation and 2) pure AmpB and ChiAmpB NLC at equivalent concentration of AmpB after 24-hour incubation]

In contrast, both ChiNLC and ChiAmpB NLC did not show any sign of haemolysis after 3-hour of incubation, showing that the carrier is biocompatible and AmpB is well-encapsulated within the nanoparticles. Upon 24-hour incubation, no haemolysis was observed for ChiNLC and ChiAmpB NLC at concentration below 25 and 12.5 µg/mL respectively. Noteworthy, the haemolytic behaviour of ChiAmpB NLC was time-dependent since the percentage haemolysis at 24-hour increased significantly as compared to the 3-hour incubation particularly at high concentration of ChiAmpB NLC (> 25 µg/mL). This phenomenon is consistent with the extended release of AmpB observed in Figure 2 which is likely to further mitigate the side effects due to AmpB. Besides, there was a linear correlation between the concentration of ChiAmpB NLC with the percentage of haemolysis in which the highest concentration of ChiAmpB NLC (100 µg/mL) marked the highest haemolysis (53.2 ± 1.6 %), which is in accordance with other studies (13,33). Nevertheless, the percentage of haemolysis of both ChiNLC and ChiAmpB NLC were significantly lower than the pure AmpB, showing that the carrier system offered 2-7 times less toxic effects on the RBC than the pure AmpB.

Figure 7 shows the cytotoxic effect of ChiAmpB NLC and drug-free ChiNLC formulations compared to Amphotret® and pure AmpB in HT-29 cell line via MTT assay.

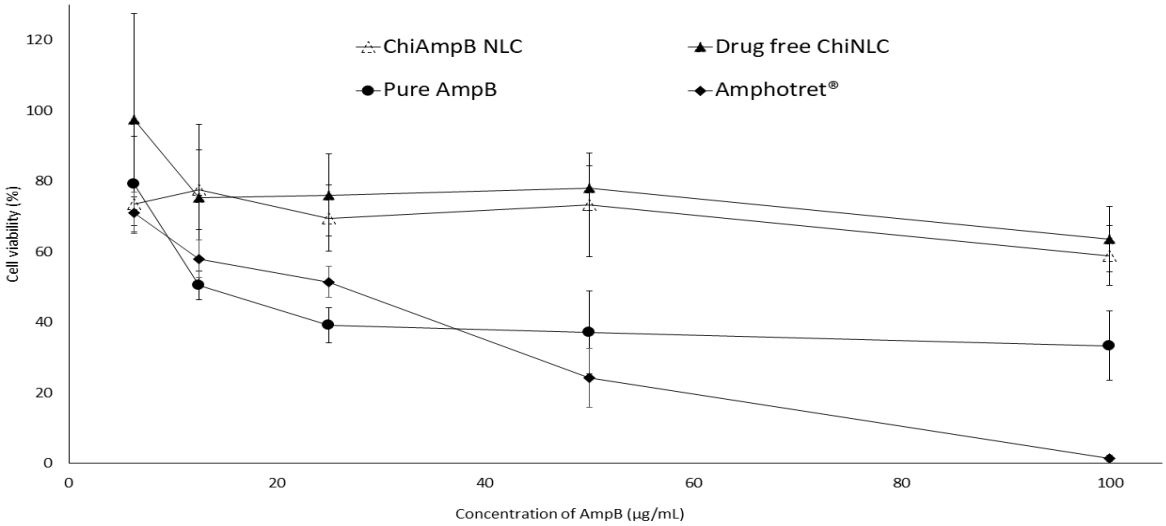

382

383 **Figure 7: Cytotoxicity of formulations after 48-hour incubation [mean ± S.D., n=3]**

384

385

386

387

388 The percentage of cell viability between ChiAmpB NLC and drug-free ChiNLC formulations were
389 almost superimposable, albeit lower cell viability was observed from ChiAmpB NLC formulation,
390 showing that the AmpB is well-encapsulated within the nanoparticles (50). This mirrors the sustained
391 release of AmpB observed in ChiAmpB NLC, where about 20% release of AmpB remained sustained
392 after 50 minutes. This slow release of AmpB is thus non-toxic to cells. The decrease in percentage of
393 cell viability was dose-dependent as 100 µg/mL of ChiAmpB NLC observed the lowest cell viability.
394 Despite the reduction in cell viability, the IC_{50} (50 % of cell growth inhibition) of ChiAmpB NLC was
395 not detected up to the highest concentration studied, 100 µg/mL (51). In contrast, the IC_{50} for pure
396 AmpB and Amphotret® were 12.5 and 25 µg/mL, respectively. Thus, we inferred that the ChiAmpB
397 NLC was at least 4-10 times less cytotoxic than the pure AmpB and Amphotret®. This outcome is
398 consistent with those from other studies (15,52,53). Besides, Amphotret® showed higher toxicity

than the pure AmpB at concentrations above 50 µg/mL in which we hypothesized that it was due to surfactant (sodium deoxycholate) present in the Amphotret® (54,55). Thus, the low cell viability observed from Amphotret® resulted from the synergistic toxicity due to AmpB and sodium deoxycholate. Hence, along with haemolysis (Figure 6) we ascertained that the ChiAmpB NLC is a well-tolerated formulation based on the biocompatibility of the excipients and polyaggregated state of AmpB reported in previous study (18,56).

CONCLUSION

The ChiAmpB NLC formulation showed the potential for further studies through its desired physical and chemical stability. The combination of chitosan and NLC exhibited good biocompatibility through its non-toxic behaviour in haemolysis and cytotoxicity assays. Besides, the intrinsic antifungal properties of AmpB remained unaffected by the formulation process or the incorporation of chitosan. The mucoadhesive behaviour of the ChiAmpB NLC ~~shows that we have~~ conclusively illustrates ~~d~~ the translation of the *in vitro* mucoadhesion data to *ex vivo* animal study. Crucially, the ChiAmpB NLC is mucoadhesive in the small intestinal region, which makes it ideal for a delayed transit and possible maximised uptake in that region.

REFERENCES

1. Lemke A, Kiderlen AF, Kayser O. Amphotericin B. Appl Microbiol Biotechnol. 2005;68:151–62.
2. Wasan EK, Bartlett K, Gershkovich P, Sivak O, Banno B, Wong Z, Gagnon J, Gates B, Leon CG, Wasan KM. Development and characterization of oral lipid-based amphotericin B formulations with enhanced drug solubility, stability and antifungal activity in rats infected with Aspergillus fumigatus or Candida albicans. Int J Pharm. 2009;372:76–84.
3. Nieto J, Alvar J, Rodríguez C, San Andrés MI, San Andrés MD, González F. Comparison of conventional and lipid emulsion formulations of amphotericin B: pharmacokinetics and toxicokinetics in dogs. Res Vet Sci. 2018;117:125–32.

4. Barwicz J, Christian S, Gruda I. Effects of the aggregation state of amphotericin B on its toxicity to mice. Antimicrob Agents Chemother. 1992;36:2310–5.

5. Butani D, Yewale C, Misra A. Topical amphotericin B solid lipid nanoparticles: design and development. Colloids Surfaces B Biointerfaces. 2016;139:17–24.

6. Santangelo R, Paderu P, Delmas G, Chen ZW, Mannino R, Zarif L, Perlin DS. Efficacy of oral cochleate-amphotericin B in a mouse model of systemic candidiasis. Antimicrob Agents Chemother. 2000;44:2356–60.

7. Nahar M, Mishra D, Dubey V, Jain NK. Development, characterization, and toxicity evaluation of amphotericin B-loaded gelatin nanoparticles. Nanomedicine: Nanotechnology, Biology, and Medicine. 2008;4:252–61.

8. Tan SW, Billa N, Roberts CR, Burley JC. Surfactant effects on the physical characteristics of amphotericin B-containing nanostructured lipid carriers. Colloids Surfaces A Physicochem Eng Asp. 2010;372:73–9.

9. Amekyeh H, Billa N, Yuen K-H, Chin SLS. A gastrointestinal transit study on amphotericin B-loaded solid lipid nanoparticles in rats. AAPS PharmSciTech. 2015;16:871–7.

10. Vaghela R, Kulkarni PK, Osmani RAM, Naga Sravan Kumar Varma V, Bhosale RR, Raizaday A, Hani U. Design, development and evaluation of mannosylated oral amphotericin B nanoparticles for anti-leishmanial therapy: oral kinetics and macrophage uptake studies. J Drug Deliv Sci Technol. 2018;43:283–94.

11. Ishaq ZA, Ahmed N, Anwar MN, ul-Haq I, ur-Rehman T, Ahmad NM, Elaissari A. Development and *in vitro* evaluation of cost effective amphotericin B polymeric emulsion. J Drug Deliv Sci Technol. 2018;46:66–73.

12. Jabri T, Imran M, Shafiullah, Rao K, Ali I, Arfan M, Shah MR. Fabrication of lecithin-gum tragacanth muco-adhesive hybrid nano-carrier system for *in-vivo* performance of

447 amphotericin B. Carbohydr Polym. 2018;194:89–96.

448 13. Espada R, Valdespina S, Alfonso C, Rivas G, Ballesteros MP, Torrado JJ. Effect of aggregation
449 state on the toxicity of different amphotericin B preparations. Int J Pharm. 2008;361:64–9.

450 14. Hamill RJ. Amphotericin B formulations: a comparative review of efficacy and toxicity. Drugs.
451 2013;73:919–34.

452 15. Silva AE, Barratt G, Cheŕon M, Egito EST. Development of oil-in-water microemulsions for the
453 oral delivery of amphotericin B. Int J Pharm. 2013;454:641–8.

454 16. Muchow M, Maincent P, Muller RH. Lipid nanoparticles with a solid matrix (SLN, NLC, LDC) for
455 oral drug delivery. Drug Dev Ind Pharm. 2008;34:1394–405.

456 17. Yoon G, Park JW, Yoon I. Solid lipid nanoparticles (SLNs) and nanostructured lipid carriers
457 (NLCs): recent advances in drug delivery. J Pharm Investig. 2013;43:353–62.

458 18. Tan Sui Ling J, Billa N, Roberts CJ. Mucoadhesive chitosan-coated nanostructured lipid carriers
459 for oral delivery of amphotericin B. Pharm Dev Technol. 2018:1–24.

460 19. Gordillo-galeano A, Mora-huertas CE. Solid lipid nanoparticles and nanostructured lipid
461 carriers : A review emphasizing on particle structure and drug release. Eur J Pharm Biopharm;
462 2018;133:285–308.

463 20. Fu T, Yi J, Lv S, Zhang B. Ocular amphotericin B delivery by chitosan modified nanostructured
464 lipid carriers for fungal keratitis targeted therapy. J Liposome Res; 2016; 27:228-33

465 21. Tripathi P, Verma A, Dwivedi P, Sharma D, Kumar V. Formulation and characterization of
466 amphotericin B loaded nanostructured lipid carriers using microfluidizer. J Biomimetics
467 Biomater Tissue Eng; 2014;4:1-4

468 22. Luo Q, Zhao J, Zhang X, Pan W. Nanostructured lipid carrier (NLC) coated with chitosan
469 oligosaccharides and its potential use in ocular drug delivery system. Int J Pharm.

2011;403:185–91.

23. Luo Y, Teng Z, Li Y, Wang Q. Solid lipid nanoparticles for oral drug delivery: chitosan coating improves stability, controlled delivery, mucoadhesion and cellular uptake. Carbohydr Polym. 2015;122:221–9.

24. Deb A, Vimala R. Camptothecin loaded graphene oxide nanoparticle functionalized with polyethylene glycol and folic acid for anticancer drug delivery. J Drug Deliv Sci Technol. 2018;43:333–42.

25. Sandri G, Motta S, Bonferoni MC, Brocca P, Rossi S, Ferrari F, Rondelli V, Cantu L, Caramella C, Favero ED. Chitosan-coupled solid lipid nanoparticles: tuning nanostructure and mucoadhesion. Eur J Pharm Biopharm. 2017;110:13–8.

26. Fonte P, Andrade F, Araújo F, Andrade C, Neves J Das, Sarmento B. Chitosan-coated solid lipid nanoparticles for insulin delivery. Methods Enzymol. 2012;508:295–314.

27. Doktorovova S, Souto EB, Silva AM. Nanotoxicology applied to solid lipid nanoparticles and nanostructured lipid carriers - a systematic review of in vitro data. Eur J Pharm Biopharm. 2014;87:1–18.

28. Garcia-Orue I, Gainza G, Girbau C, Alonso R, Aguirre JJ, Pedraz JL, Igartua M, Hernandez RM. LL37 Loaded nanostructured lipid carriers (NLC): a new strategy for the topical treatment of chronic wounds. Eur J Pharm Biopharm. 2016; 108:310-16.

29. Khan MA, Zafaryab M, Mehdi SH, Quadri J, Rizvi MMA. Characterization and carboplatin loaded chitosan nanoparticles for the chemotherapy against breast cancer *in vitro* studies. Int J Biol Macromol. 2017;97:115–22.

30. Bonferoni MC, Sandri G, Ferrari F, Rossi S, Larghi V, Zambito Y, Caramella C. Comparison of different *in vitro* and *ex vivo* methods to evaluate mucoadhesion of glycol-palmitoyl chitosan micelles. J Drug Deliv Sci Technol. 2010;20:419–24.

494 31. Alkhader E, Billa N, Roberts CJ. Mucoadhesive chitosan-pectinate nanoparticles for the
495 delivery of curcumin to the colon. AAPS PharmSciTech. 2016;18:1–10.

496 32. Jung SH, Lim DH, Jung SH, Lee JE, Jeong K-S, Seong H, Shim BC. Amphotericin B-entrapping
497 lipid nanoparticles and their *in vitro* and *in vivo* characteristics. Eur J Pharm Sci. 2009;37:313–
498 20.

499 33. Radwan MA, AlQuadeib BT, Šiller L, Wright MC, Horrocks B. Oral administration of
500 amphotericin B nanoparticles: antifungal activity, bioavailability and toxicity in rats. Drug
501 Deliv. 2017;24:40–50.

502 34. Vieira ACC, Chaves LL, Pinheiro S, Pinto S, Pinheiro M, Lima SC, Ferreira D, Sarmento B, Reis S.
503 Mucoadhesive chitosan-coated solid lipid nanoparticles for better management of
504 tuberculosis. Int J Pharm. 2018;536:478–85.

505 35. Aditya NP, Macedo AS, Doktorovova S, Souto EB, Kim S, Chang PS, Ko S. Development and
506 evaluation of lipid nanocarriers for quercetin delivery: a comparative study of solid lipid
507 nanoparticles (SLN), nanostructured lipid carriers (NLC), and lipid nanoemulsions (LNE). LWT -
508 Food Sci Technol. 2014;59:115–21.

509 36. Abdelwahed W, Degobert G, Stainmesse S, Fessi H. Freeze-drying of nanoparticles:
510 formulation, process and storage considerations. Adv Drug Deliv Rev. 2006;58:1688–713.

511 37. Kumar V, Adamson DH., Prud'homme RK. Fluorescent polymeric nanoparticles: aggregation
512 and phase behavior of pyrene and amphotericin B molecules in nanoparticle cores. Small.
513 2010;6:2907–14.

514 38. Drin G, Cottin S, Blanc E, Rees AR, Temsamani J. Studies on the internalization mechanism of
515 cationic cell-penetrating peptides. J Biol Chem. 2003;278:31192–201.

516 39. Gartziandia O, Herran E, Pedraz JL, Carro E, Igartua M, Hernandez RM. Chitosan coated
517 nanostructured lipid carriers for brain delivery of proteins by intranasal administration.

518 Colloids Surfaces B Biointerfaces; 2015;134:304–13.

519 40. Tiwari R, Pathak K. Nanostructured lipid carrier versus solid lipid nanoparticles of simvastatin:
520 Comparative analysis of characteristics, pharmacokinetics and tissue uptake. Int J Pharm;
521 2011;415:232–43.

522 41. Khosa A, Reddi S, Saha RN. Nanostructured lipid carriers for site-specific drug delivery.
523 Biomed Pharmacother; 2018;103:598–613.

524 42. Weber S, Zimmer A, Pardeike J. Solid lipid nanoparticles (SLN) and nanostructured lipid
525 carriers (NLC) for pulmonary application : a review of the state of the art. Eur J Pharm
526 Biopharm; 2014;86:7–22.

527 43. Souza ACO, Nascimento AL, de Vasconcelos NM, Jerônimo MS, Siqueira IM, R-Santos L, Cintra
528 DOS, Fuscaldi LL, Pires Junior OR, Titze-de-Almeida R, Borin MF, Bao SN, Martins OP, Cardoso
529 VN, Fernandes SO, Mortari MR, Tedesco AC, Amaral AC, Felipe MSS, Bocca AL. Activity and *in*
530 *vivo* tracking of amphotericin B loaded PLGA nanoparticles. Eur J Med Chem. 2015;95:267–
531 76.

532 44. Jain V, Gupta A, Pawar VK, Asthana S, Jaiswal AK, Dube A, Chourasia MK. Chitosan-assisted
533 immunotherapy for intervention of experimental leishmaniasis via amphotericin B-loaded
534 solid lipid nanoparticles. Appl Biochem Biotechnol. 2014;174:1309–30.

535 45. Das S, Ghosh S, De AK, Bera T. Oral delivery of ursolic acid-loaded nanostructured lipid carrier
536 coated with chitosan oligosaccharides: development, characterization, *in vitro* and *in vivo*
537 assessment for the therapy of leishmaniasis. Int J Biol Macromol. 2017;102:996–1008.

538 46. Cauchetier E, Deniau M, Fessi H, Astier A, Paul M. Atovaquone-loaded nanocapsules:
539 influence of the nature of the polymer on their *in vitro* characteristics. 2003;250:273–81.

540 47. Mora-Huertas CE, Fessi H, Elaissari A. Polymer-based nanocapsules for drug delivery. Int J
541 Pharm. 2010;385:113–42.

542 48. Bhattacharjee S. DLS and zeta potential – What they are and what they are not? J Control
543 Release. 2016;235:337–51.

544 49. Bansil R, Turner BS. Mucin structure, aggregation, physiological functions and biomedical
545 applications. Curr Opin Colloid Interface Sci. 2006;11:164–70.

546 50. Ying XY, Cui D, Yu L, Du YZ. Solid lipid nanoparticles modified with chitosan oligosaccharides
547 for the controlled release of doxorubicin. Carbohydr Polym. 2011;84:1357–64.

548 51. Ridolfi DM, Marcato PD, Justo GZ, Cordi L, Machado D, Durán N. Chitosan-solid lipid
549 nanoparticles as carriers for topical delivery of tretinoin. Colloids Surfaces B Biointerfaces.
550 2012;93:36–40.

551 52. Caldeira LR, Fernandes FR, Costa DF, Frezard F, Afonso LCC, Ferreira LAM. Nanoemulsions
552 loaded with amphotericin B: a new approach for the treatment of leishmaniasis. Eur J Pharm
553 Sci. 2015;70:125–31.

554 53. Senna JP, Barradas TN, Cardoso S, Castiglione TC, Serpe MJ, Silva KG de H, Mansur CRE. Dual
555 alginate-lipid nanocarriers as oral delivery systems for amphotericin B. Colloids Surfaces B
556 Biointerfaces. 2018;166:187–94.

557 54. Sakai M, Imai T, Ohtake H, Otagiri M. Cytotoxicity of absorption enhancers in caco-2 cell
558 monolayers. J Pharm Pharmacol. 1998;50:1101–8.

559 55. Italia JL, Yahya MM, Singh D, Ravi Kumar MN V. Biodegradable nanoparticles improve oral
560 bioavailability of amphotericin B and show reduced nephrotoxicity compared to intravenous
561 fungizone®. Pharm Res. 2009;26:1324–31.

562 56. Ramalingam P, Ko YT. Improved oral delivery of resveratrol from N-trimethyl chitosan-g-
563 palmitic acid surface-modified solid lipid nanoparticles. Colloids Surfaces B Biointerfaces.
564 2016;139:52–61.

565